



# Simulation research of a counter-flow rotary kiln hazardous waste incineration system

Shiqiao Yang<sup>1,2</sup> · Qingfeng Kong<sup>1</sup> · Dewang Zeng<sup>1</sup> · Shiliang Wu<sup>1</sup> · Feng Gong<sup>1</sup> · Rui Xiao<sup>1</sup>

Received: 16 December 2021 / Accepted: 18 June 2022  
© The Author(s) 2022

## Abstract

As industrialization accelerates and the amount of hazardous waste generated gradually increases, the means of disposal of hazardous waste is of increasing concern. In this paper, a 40 t/d counter-flow rotary kiln incineration system owned by a Jiangsu environmental protection company was researched. The software Aspen Plus was used to build the mixed pyrolysis model and the software Fluent was used to build the computational fluid dynamics model of the incineration system. The influence of the calorific value of the hazardous waste, the operating temperature and the air supply on the operational effectiveness of the incineration system were analyzed by varying the simulation conditions. The results show that the SO<sub>x</sub> and NO<sub>x</sub> content of the product is lower when the operating temperature is above 800 °C. The incineration system could only operate above 800 °C when the calorific value of the hazardous waste is not less than 1500 kcal/kg. The incineration system operated best at a primary air velocity of 1.5 m/s. The simulation results in this paper serve as a guide for the operation of counter-flow rotary kiln incineration systems.

**Keywords** Hazardous waste · Count-flow rotary kiln · Aspen plus · Fluent · Simulation

## 1 Introduction

Since the reform and opening-up, all industries in China have been developing rapidly and the economic level has greatly improved. However, the issue of environmental pollution is also increasingly serious (Nanda and Berruti 2021). Regarding pollutants, hazardous waste is considered as one of the most difficult wastes to address due to its reactivity, flammability, toxicity and corrosiveness. In addition, hazardous waste is extremely harmful to both people and the environment, whereby it can endanger human health (Tekade 2021) and cause serious damage to soil (Wang and Geng 2015) and water bodies (Hadas et al. 2021; Visvanathan 1996). Therefore, an efficient and safe disposal of hazardous waste is essential.

Hazardous waste treatment methods include physical and chemical methods, solidification, safe landfill, and incineration (Makarichi et al. 2018; Paula et al. 1998; Singhbhandhu and Tezuka 2010). Among these, physical and chemical methods cannot completely treat hazardous waste and still require a conjunction with other treatment methods (Huang et al. 1993; Murphy and McAllister 2001). Solidification and safe landfill methods are simple to operate, however, they have long treatment cycles and cannot achieve a rapid and effective treatment of large quantities of hazardous waste (Conner and Hoeffner 1998; Malviya and Chaudhary 2006). Incineration is the most widely used method due to its high efficiency and thorough treatment. The choice of a suitable incinerator is a key factor in determining the effectiveness of incineration. In order to adapt to the complex and variable composition of hazardous waste, rotary kiln incinerators, with a wide range of applications, are often used.

Liu et al. (2005) used experimental and simulation methods to research the main factors affecting the movement characteristics of hazardous waste in a rotary kiln. The results showed that the rotational speed and inclination angle of the rotary kiln affect the residence time and filling rate of hazardous waste in the rotary kiln, which, in turn, affects the actual operating effect of the rotary kiln.

✉ Rui Xiao  
ruixiao@seu.edu.cn

<sup>1</sup> Key Laboratory of Energy Thermal Conversion and Control of Ministry of Education, School of Energy and Environment, Southeast University, Nanjing 210096, China

<sup>2</sup> Everbright Environmental Protection Technology Equipment (Changzhou) Co., Ltd., Changzhou 213011, China

Andréa et al. (1998) researched the practical effect of co-processing hazardous waste treatment in cement kilns and showed that hazardous waste can act as a secondary fuel required for cement kiln incineration, where the incineration efficiency of hazardous waste was greater than 99%. The durability of the refractory in the rotary kiln is the key to the operational life of the rotary kiln. Adrian et al. (2016) conducted an experimental study on the causes of refractory brick breakage in rotary kilns, which showed that the breakage of refractory bricks was not due to thermochemical corrosion, but rather to the penetration of molten material into the refractory bricks in the rotary kiln. Then, they developed a mullite-zirconia composite as a new refractory material, which had excellent durability (Adrian et al. 2021). Zhang and Wang (2022) experimentally investigated the operating effect of rotary kilns under different hazardous waste dispensing conditions and showed that the lower the ignition temperature of the hazardous waste, the more stable the operation of the rotary kiln. Wajda et al. (2022) provided an algorithmic procedure for solving the optimal operating conditions of rotary kilns to achieve the highest energy use efficiency. A comparative analysis of the evolution of hydrocarbon composition in pilot rotary kiln incinerators and rotary kiln incinerators was carried out by Lester et al. (1991). The results showed that the experimental results in the pilot reactor were consistent with the actual operation of the rotary kiln incinerator and that the pilot system exhibited a good response to the actual operation of the rotary kiln. The incineration of hazardous waste in the rotary kiln produced dioxins and other harmful substances.

The above studies were very informative, though they did not provide a good explanation for the incomplete burning of hazardous waste and the uneven temperature distribution in rotary kilns, which often occurs in rotary kilns. The matching of the primary air volume to the calorific value of the hazardous waste was the key to the uniformity of the rotary kiln temperature, which affected the incineration of hazardous waste. The software Aspen Plus was widely used to simulate pyrolysis and gasification processes of coal and solid waste (Ismail et al. 2020). In addition, the operating temperature of the rotary kiln and the secondary combustion chamber affected pollutant emissions. Hence, a 40 t/d counter-flow rotary kiln incineration system owned by a Jiangsu environmental protection company was researched. The software Aspen Plus was used to model the mixed pyrolysis of hazardous waste in a rotary kiln and to analyze the content of pollutants such as  $\text{SO}_x$  and  $\text{NO}_x$  in the gaseous products at different temperatures. The software Fluent was used to simulate the temperature distribution and the concentration distribution of various substances in the rotary kiln and second combustion chamber. The effect of primary air flow and the calorific value

of the hazardous waste on the operation of the rotary kiln was also researched. The simulation results were of certain significance for the actual operation of rotary kilns.

## 2 Simulation methods

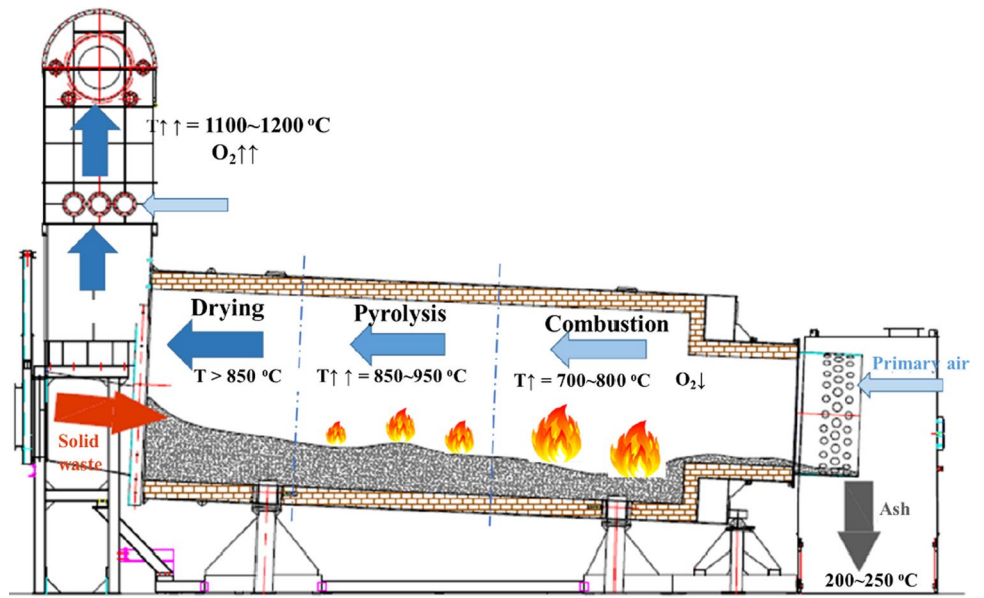
### 2.1 Introduction to counter-flow rotary kiln incineration systems

Figure 1 shows a schematic diagram of a counter-flow rotary kiln with a horizontal inclination of  $2.5^\circ$  and a rotational speed of 0.2–0.5 r/min. Hazardous waste was used as the incineration material. The component content of the hazardous waste is given in Table 1. The hazardous waste entered the rotary kiln from the kiln head and moved from the kiln head to the kiln tail under the rotation of the rotary kiln, during which the hazardous waste underwent drying, pyrolysis and combustion processes in turn, and the ash was discharged from the kiln tail. The primary air entered the rotary kiln at the end of the kiln, where it was first pre-heated by the ash, and then participated in the combustion, pyrolysis and drying processes of the hazardous waste in turn, before forming a mixture that entered the second combustion chamber.

### 2.2 Aspen plus modeling

In this paper, a hybrid pyrolysis model for the counter-flow rotary kiln incineration system was simulated using the Aspen Plus software. Three processes of drying, pyrolysis and combustion occurred sequentially in the rotary kiln, so the hybrid pyrolysis model was built by first creating a single model for each process and then connecting the single models based on the direction of material and energy flow between the models. As shown in Fig. 2, the model consisted of 13 unit operation modules, 20 material flow units (black solid line) and 6 energy flow units (red dashed line), which enabled a counter-flow reaction process between the hazardous waste and primary air in the kiln. The energy was supplied from the combustion model to the drying and pyrolysis models through the counter flow of the energy. The model contained a total of five reactors and the operating conditions for the five reactors are given in Table 2. The components of hazardous waste were complex and the chemical reactions involved in the pyrolysis and incineration of hazardous waste were numerous. Therefore, a Gibbs reactor was used to simulate the generation of various gaseous and solid products, which followed the Gibbs free energy minimum principle.

**Fig. 1** Schematic diagram of the counter-flow rotary kiln system



**Table 1** Component contents of the hazardous waste

C (%)	H (%)	O (%)	N (%)	S (%)	Moisture (%)	Ash (%)	Total (%)
36.73	0.58	7.93	3.04	4.94	14.50	32.80	100

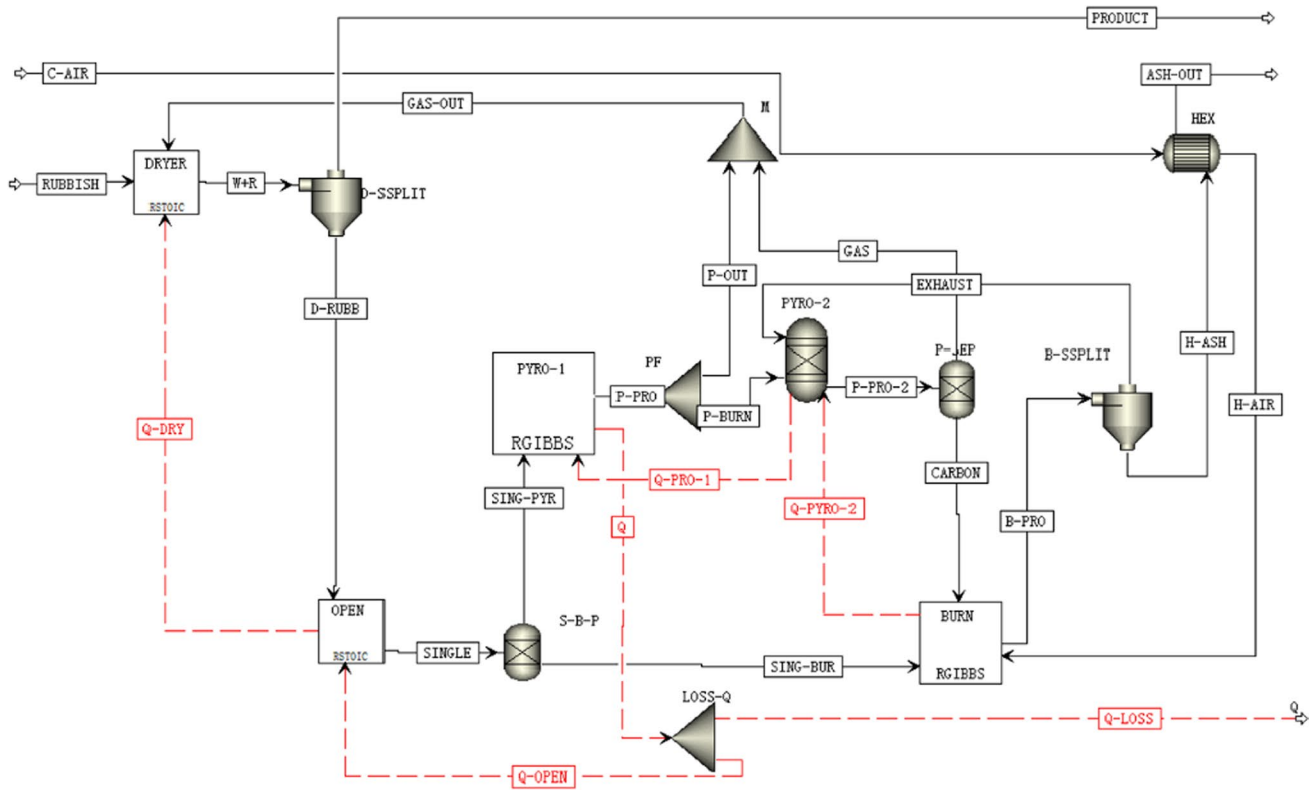


**Fig. 2** Hybrid pyrolysis model of the counter-flow rotary kiln incineration system

**Table 2** Operating conditions of each reactor

Operating conditions	Reactor modules				
	DYRER	OPEN	PYRO-1	PYRO-2	BURN
Temperature (°C)	850–900	900	900	900	950
Pressure (MPa)	0.101	0.11	0.101	0.101	0.101

## 2.3 Fluent modeling

In this paper, a CFD model of the counter-flow rotary kiln incineration system was developed using the software Fluent. The physical properties of the hazardous waste were defined in the UDF user-defined mode in Fluent, so that it existed as a “pseudo-fluid”. By setting up the pyrolysis gasification reaction of the material in the flow field area of the kiln, the pyrolysis and combustion reactions of the hazardous waste occurred on a time scale appropriate to the kiln. The pyrolysis and combustion reactions of hazardous waste were adapted to the time scale of the kiln. The component transport model was used to simulate the flow of each component and pyrolysis gas in the kiln, resulting in the simultaneous simulation of the gas–solid two-phase flow, the pyrolysis process of solid materials and the combustion process of materials and pyrolysis gas throughout the kiln.

### 2.3.1 Geometric model and boundary conditions

The geometry of the counter-flow rotary kiln is shown in Fig. 3. It can be seen that the number of inlets and outlets of the rotary kiln was four, divided into the following four categories: material inlet, primary air inlet, mixed gas outlet and slag outlet. The boundary conditions for each inlet and outlet are given in Table 3.

**Table 3** CFD model boundary conditions

Phase	Types of boundary conditions	Given parameters
Hazardous waste inlet	Mass flow rate (kg/s)	0.463
	Temperature (K)	300
Primary wind inlet	Primary wind speed (m/s)	1.5
	Turbulence intensity (%)	5
	Temperature (K)	300
Ash outlet	Gauge pressure (Pa)	0
Mixture outlet	Gauge pressure (Pa)	− 50

### 2.3.2 Mathematical-physical model

In the CFD model, the standard  $k$ – $\epsilon$  model was chosen as the turbulent flow model and a component transport model was used to simulate the chemical reaction process. Only volumetric reactions were considered in the model and the effects of energy diffusion and thermal diffusion on the reaction were considered.

#### (1) Turbulence model.

The equation of turbulent kinetic energy  $k$  was as follows:

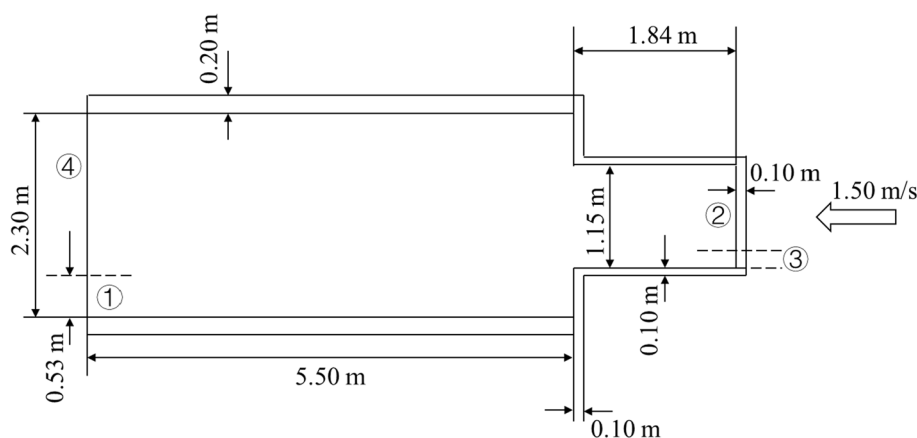
$$\frac{\partial}{\partial t}(\rho_d k) + \nabla(\rho_d v_d k) = \nabla \left( \frac{\mu_{td}}{\sigma_k} \nabla \cdot k \right) + G_{kd} - \rho_d \epsilon \quad (1)$$

The equation of turbulent energy dissipation rate  $\epsilon$  was as follows:

$$\frac{\partial}{\partial t}(\rho_d \epsilon) + \nabla(\rho_d v_d \epsilon) = \nabla \left( \frac{\mu_{td}}{\sigma_k} \nabla \cdot \epsilon \right) + \frac{\epsilon}{k} (C_{1e} G_{kd} - C_{2e} \rho_d \epsilon) \quad (2)$$

where  $t$  is the time,  $\rho_d$  is the density of the mixture,  $v_d$  is the speed of the mixture,  $\mu_{td}$  is the turbulent viscosity of the mixture,  $G_{kd}$  is the turbulent energy, and  $C_{1e}$ ,  $C_{2e}$ ,  $\sigma_k$  and  $\sigma_\epsilon$  are turbulence model coefficients.

#### (2) Mathematical model of fluid dynamics.

**Fig. 3** Schematic diagram of the geometric of the counter-flow rotary kiln

The reaction equations for material and fluid dynamics in a rotary kiln generally included four equations for the conservation of mass, the conservation of momentum, the conservation of energy and the conservation of component transport.

$$\frac{\partial \rho}{\partial t} + \nabla(\rho u) = S_p \quad (3)$$

$$\frac{\partial(\rho u)}{\partial t} + \nabla(\rho u \cdot u) = -\nabla p + \nabla(\mu \nabla u) + S_N \quad (4)$$

$$\frac{\partial(\rho u)}{\partial t} + \nabla(\rho u \cdot H) = \nabla(\lambda \nabla T) + S_H \quad (5)$$

$$\frac{\partial(\rho Y_f)}{\partial t} + \nabla(\rho u \cdot Y_f) = \nabla(D \nabla(Y_f)) + S_Y + R_f \quad (6)$$

where  $\rho$  is the density,  $\rho'$  is the average density,  $u'$  is the instantaneous speed,  $p$  is the individual gas partial pressure,  $\mu$  is the kinetic viscosity,  $H$  is the specific enthalpy of fluids,  $T$  is the temperature,  $\lambda$  is the thermal conductivity of fluids,  $Y_f$  is the mass fraction,  $D$  is the diffusion coefficient,  $R_f$  is the production rate of components per unit volume, and  $S_p$ ,  $S_N$ ,  $S_H$  and  $S_Y$  are source items.

(3) Chemical reaction model.

Seven chemical reactions were initially set up in the simulation. The chemical reactions were calculated using the Arrhenius rate model set up with the equation:

$$K = A \exp\left(-\frac{Ea}{RT}\right) \quad (7)$$

where  $K$  is the Arrhenius constant,  $A$  is the pre-exponential factor,  $Ea$  is the activation energy, and  $R$  is the molar gas constant.

The main reaction equations and kinetic parameters are given in Table 4.

### 3 Simulation results and analysis

#### 3.1 Grid independence test and model validation

The grid independence of the CFD model was checked using the temperature distribution in the rotary kiln at 1.5 m/s as a test indicator. The grid shape was rectangular and the grid quality is given in Table 5.

Figure 4 shows the results of the independence test for the grid. It can be observed that the temperature distribution was too far from the expected error when using 900,000 grids, while the simulation with 950,000 grids exhibited the most consistent temperature distribution, as expected. When the number of grids was increased to one million, the temperature distribution curve was also very close to

**Table 4** Main reaction equations and kinetic parameters

Reactions	$Ea$ (J/mol)	$A$
$2CO + O_2 \rightarrow 2CO_2$	$1.70 \times 10^5$	$2.24 \times 10^{-11}$
$C + O_2 \rightarrow 2CO$	$1.67 \times 10^5$	$3.00 \times 10^{-7}$
$C + H_2O \rightarrow CO + H_2$	$7.00 \times 10^4$	$3.00 \times 10^{-9}$
$2C + 2H_2 \rightarrow C_2H_4$	$3.00 \times 10^4$	$1.00 \times 10^{-7}$
$C + 2H_2 \rightarrow CH_4$	$2.00 \times 10^4$	$6.00 \times 10^{-9}$
$H_2O(l) \rightarrow H_2O(g)$	$1.00 \times 10^3$	$1.00 \times 10^{-11}$
$CH_4 + 2O_2 \rightarrow CO_2 + 2H_2O$	$2.03 \times 10^5$	$2.12 \times 10^{-10}$

**Table 5** Grid quality

Number of grids	Grid size (m <sup>2</sup> )	Grid quality
900,000	$1.21 \times 10^{-5}$	Greater than 0.381
950,000	$1.14 \times 10^{-5}$	Greater than 0.517
1,000,000	$1.09 \times 10^{-5}$	Greater than 0.494

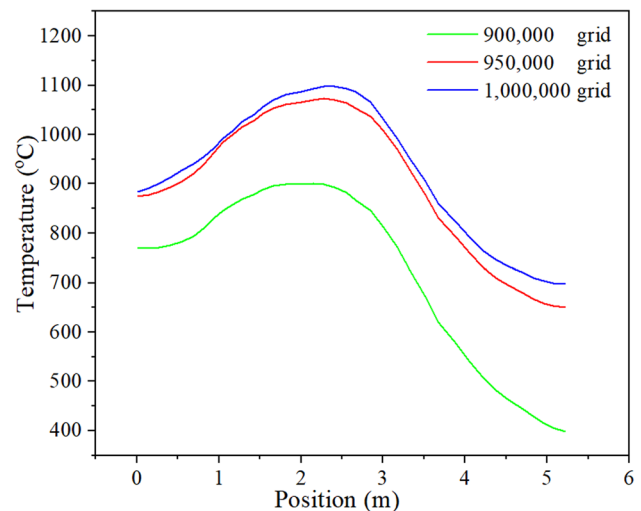


**Fig. 4** Results of the grid independence test for the temperature field

the expected distribution, but at this point, the error from the expected distribution was already small. The number of grids should be as small as possible for the simulation to meet our expectations, so from this grid independence check, it can be determined that a grid of 950,000 should be chosen.

In the actual operation of a counter-flow rotary kiln system, the average temperature in the rotary kiln was approximately 950 °C, with high temperatures in the middle of the kiln and low temperatures on the sides. In the temperature distribution of the rotary kiln shown in Fig. 4, the middle temperature was high and the two sides were low, which was consistent with the actual operating results of the rotary kiln. The average temperature was approx. 950 °C. Hence,

the CFD model of the counter-flow rotary kiln incineration system was accurate.

### 3.2 Calculation of mass balance and energy balance

The PR-BM method was chosen in Aspen Plus to simulate the pyrolysis incineration process of hazardous waste, and mass-energy accounting was carried out using the following method.

$$M_{\text{loss}} = M_{\text{hw}} + M_{\text{air}} - M_{\text{fg}} + M_{\text{ash}} \quad (8)$$

$$E_{\text{loss}} = E_{\text{hw}} + E_{\text{air}} - E_{\text{fg}} - E_{\text{ash}} \quad (9)$$

where,  $M_{\text{loss}}$  represents the mass loss in rotary kilns;  $M_{\text{hw}}$  and  $M_{\text{air}}$  represent the mass flow of hazardous waste and air, respectively;  $M_{\text{fg}}$  and  $M_{\text{ash}}$  represent the mass flow of flue gas and ash, respectively;  $E$  represents the energy of the various components.

To make the model more realistic for engineering purposes, a mass loss of 1% and a heat loss of 2% were considered in the aspen modelling. A mass and energy balance using the simulation results showed that  $M_{\text{loss}}$  and  $E_{\text{loss}}$  were 16.67 kg/h and 123,333 kcal/h, respectively. The above results satisfied the mass and energy balance.

### 3.3 Effect of operating temperature

The yields of reducing gases, sulfides and nitrides obtained from mixed pyrolysis model simulations at 500–900 °C are given in Fig. 5. It can be seen that with the increase of operating temperature, the contents of CO and H<sub>2</sub> in the mixed gas gradually increased, but the contents of CH<sub>4</sub> gradually decreased. With the increase of the operating temperature, the proportion of H<sub>2</sub>S in gaseous sulfides increased and the proportion of SO<sub>2</sub> decreased. The proportion of HCN and NH<sub>3</sub> increased and the proportion of NO decreased. SO<sub>2</sub> and NO were mainly produced by the combustion of fuel. The kiln tail had sufficient air and high temperatures to facilitate the production of sulfur SO<sub>x</sub> and NO<sub>x</sub>.

The drying and pyrolysis of hazardous waste occurred in the front and middle sections of the rotary kiln, while air was fed from the tail section of the kiln. Therefore, there was insufficient air during the pyrolysis of hazardous waste. Therefore, it could be assumed that as the reaction temperature increased, more N and S elements in the hazardous waste participated in the pyrolysis reaction to form H<sub>2</sub>S, NH<sub>3</sub> and HCN. The result led to a reduction in the proportion of SO<sub>x</sub> and NO<sub>x</sub> in the mixture. In addition, as can be seen in Fig. 5, the yield of various reducing gases tended to be stable, the contents of SO<sub>x</sub> and NO<sub>x</sub> were lower, and the emission of pollutants reached a stable level when the operating temperature was above 800 °C. Therefore, the

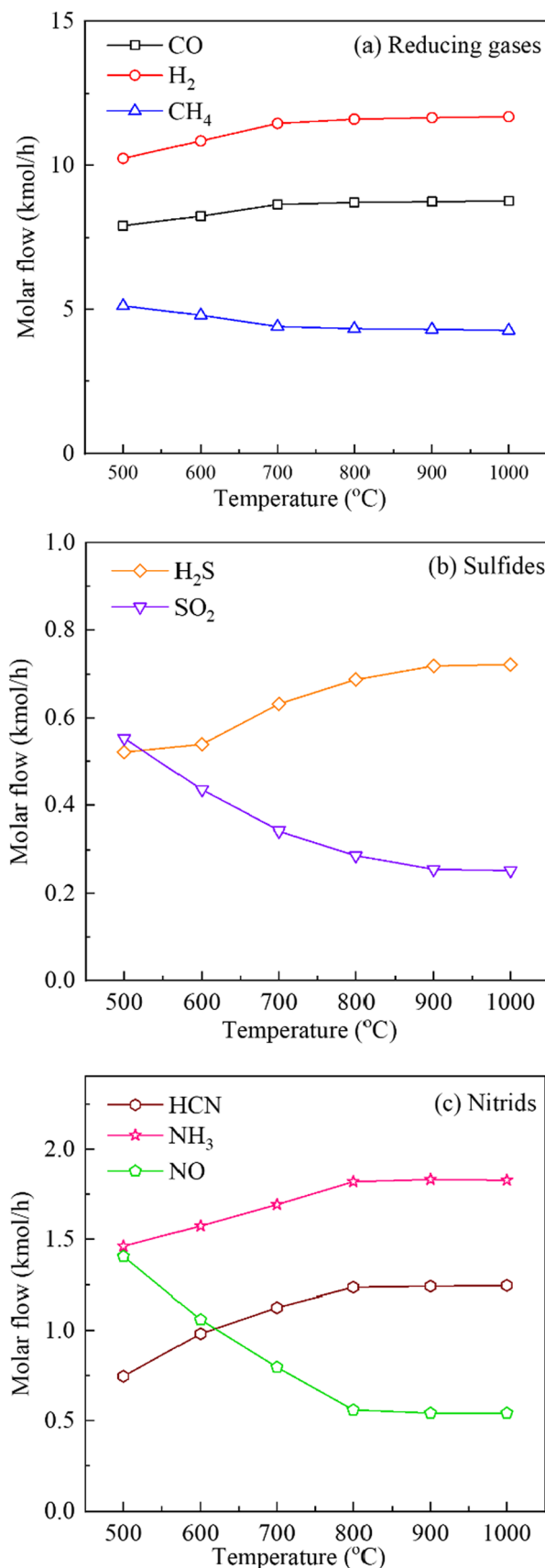


Fig. 5 Pyrolysis of materials at different temperatures

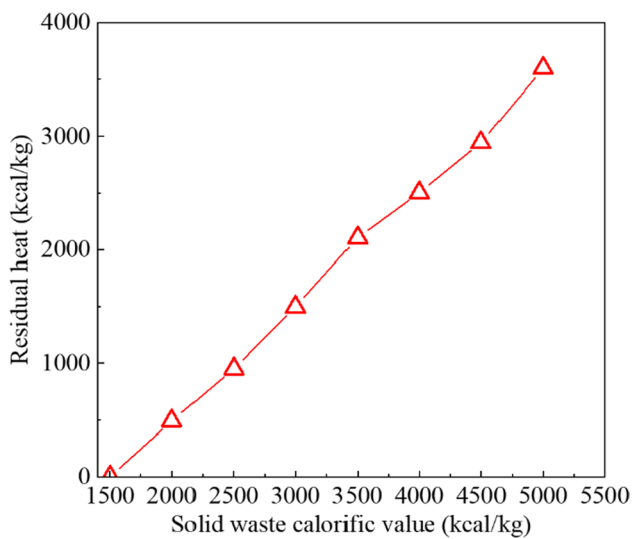


Fig. 6 Residual heat in the gas mixture

operating temperature should be higher than 800 °C in the actual operation of the counter-flow rotary kiln system.

### 3.4 Effect of the hazardous waste calorific value

When the calorific value of the hazardous waste was low, there was a risk that the counter-flow rotary kiln incineration system could not reach 800 °C. The high level of gaseous pollutants generated by the operation of the system indicated that the hazardous could not be incinerated in the counter-flow rotary kiln. Hence, the actual operation of the counter-flow rotary kiln incineration system was simulated using a mixed pyrolysis model with hazardous waste of different calorific values. Figure 6 shows the calorific values (residual heat) of the reducing gases in the gas mixture obtained from the simulated operation of the mixed pyrolysis model for hazardous waste with calorific values in the range of 1000 kcal/kg to 5000 kcal/kg. Residual heat is the amount of heat that can be released by complete combustion of the combustible gas in the exit gas of the rotary kiln. The simulation results obtained from the mixed pyrolysis model showed that the main flammable gases in the flue gas were CO, H<sub>2</sub> and CH<sub>4</sub>. Hydrocarbon gases with C > 2 were less than five per cent of the total flammable gas. Thus, only H<sub>2</sub>, CO and CH<sub>4</sub> were considered when calculating the residual heat of the mixture. The calculation formula was as follows:

$$Q = V_{H_2} \cdot q_{H_2} + V_{CO} \cdot q_{CO} + V_{CH_4} \cdot q_{CH_4} \quad (10)$$

where  $Q$  is the residual heat,  $V_{H_2}$ ,  $V_{CO}$  and  $V_{CH_4}$  are the gas volumes, and  $q_{H_2}$ ,  $q_{CO}$  and  $q_{CH_4}$  are the calorific values.

The total energy consumption, the calorific value of hazardous waste and the total residual heat satisfied the following equation:

$$\text{Residual heat} = \text{Calorific value of hazardous waste} \\ - \text{Energy consumption}$$

As can be seen from Fig. 6, when the hazardous waste calorific value was 1500 kcal/kg, the residual heat in the mixture entering the second combustion chamber was 3.65 kcal/kg, which indicated that the counter-flow rotary kiln incineration system could satisfy its own energy balance at an operating temperature of 850 °C. The result indicated that the calorific value of 1500 kcal/kg was the critical value at 850 °C.

### 3.5 Effect of primary air volume and primary air speed

Most of the existing rotary kiln incineration systems use the negative pressure suction air supply method. In the actual operation, the primary air volume and velocity are difficult to control, making the rotary kiln incineration system less stable. Therefore, the CFD model was used to adjust the primary air supply method to active air supply, and the primary air volume and speed were adjusted to investigate the effect of primary air volume and speed on the counter-flow rotary kiln incineration system.

The cross-sectional area of the air inlet was constant. When the primary air velocity was adjusted to 1.2 m/s, 1.5 m/s and 2.0 m/s, the corresponding air flows were 4560 Nm<sup>3</sup>/s, 5700 Nm<sup>3</sup>/s and 7600 Nm<sup>3</sup>/s, respectively. Figure 7 shows the temperature and CO concentration distributions inside the rotary kiln for the three air velocities mentioned above, respectively. H<sub>2</sub>, CO and CH<sub>4</sub> were all mainly produced in the pyrolysis zone of the rotary kiln, with rotary kiln pyrolysis occurring mainly in the middle section of the rotary kiln. Therefore, the effect of primary air volume and primary air velocity on the distribution of H<sub>2</sub> and CH<sub>4</sub> concentrations was similar to CO. Therefore, their concentration distribution can be referred to that of CO.

As can be seen from Fig. 7a, the variation in air speed had a significant effect on the overall temperature distribution in the kiln. The high temperature region of the rotary kiln gradually moved towards the rotary kiln inlet, when the primary air speed gradual increased. In addition, with the gradual increase in primary air volume, the kiln tail temperature gradually decreased due to the increased heat absorption by cold air. When the temperature of the rotary kiln was too low, the ash was not burned completely and, thus, the burning effect of the rotary kiln was reduced. Therefore, it was not reasonable to supply the rotary kiln with air at a speed of 2.0 m/s. As can be seen from Fig. 7b, the high concentration region of CO showed

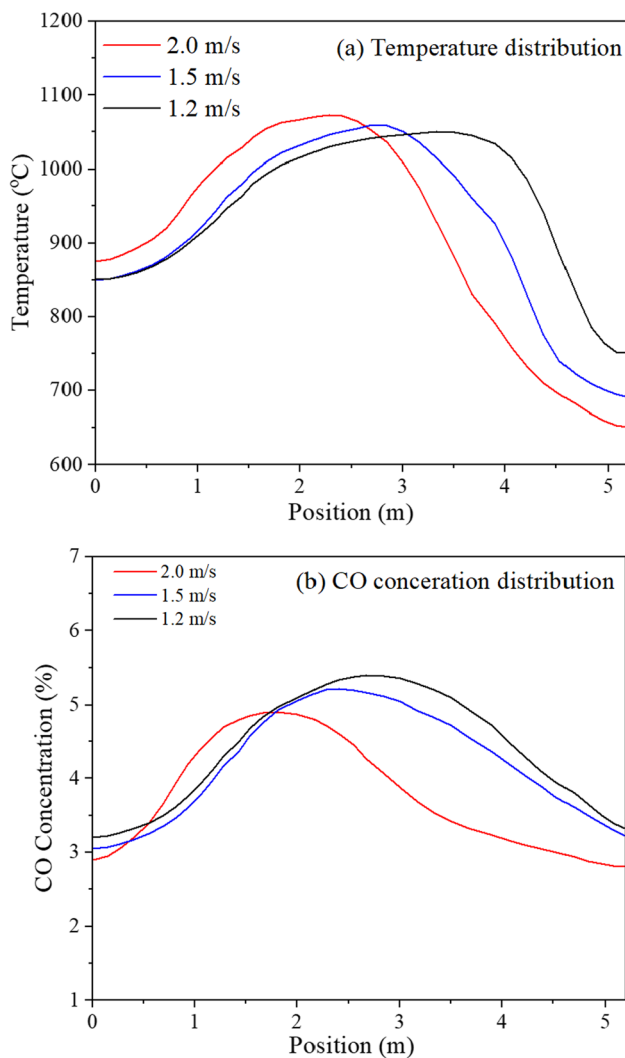


**Fig. 7** Simulation results at different wind speeds

the same characteristics as the high temperature region, both moving to the left of the rotary kiln as the primary air velocity increased. In addition, the increase in primary air volume was beneficial for the incineration of hazardous waste, resulting in a gradual reduction in the CO concentration in the rotary kiln. Therefore, hazardous waste was burned better at a wind speed of 1.5 m/s compared to 1.2 m/s.

In general, 1.5 m/s was the optimum air supply speed for a counter-flow rotary kiln incineration system, which corresponded to a primary air flow of 5700 Nm<sup>3</sup>/s.

### 3.6 Simulation results for the second combustion chamber

The simulation results of the rotary kiln showed that the combustible gases entering the second combustion chamber were mainly H<sub>2</sub>, CO and CH<sub>4</sub>. In addition, CH<sub>4</sub> was used to supplement the combustion in order to achieve an

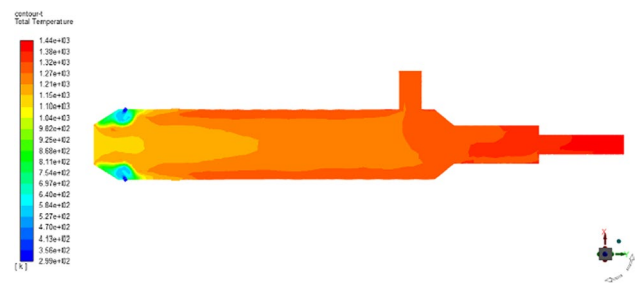


**Fig. 8** Temperature distribution in the second combustion chamber

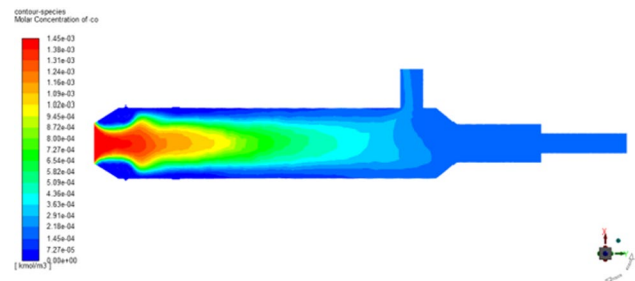


**Fig. 9** Distribution of CO concentrations in the second combustion chamber

exhaust gas temperature of more than 1150 °C. As a result, there was no significant production of SO<sub>x</sub> and NO<sub>x</sub> in the secondary combustion chamber. Therefore, the distribution of temperature and CO concentration in the second combustion chamber were given. Figure 8 shows the temperature distribution in the second combustion chamber.

The temperature at the entrance to the second combustion chamber was low, which was related to the lower flue gas temperature at the exit of the rotary kiln and the addition of supplementary fuel. However, the combustion of combustible gases in the flue gas and the make-up fuel further rose the temperature in the secondary combustion chamber, resulting in a greater temperature at the outlet of the secondary combustion chamber compared to the industry emission standard of 1100 °C.

Figure 9 shows the distribution of CO concentrations in the second combustion chamber. The concentration of CO in the secondary combustion chamber gradually decreased along the outlet direction. The rotary kiln outlet gas contained a certain amount of CO, which resulted in the highest CO concentration at the inlet of the second combustion chamber. Under the conditions of adding supplementary fuel to fuel the combustion, the CO in the second combustion chamber gradually decreased in the direction of the flue gas flow and was reduced to a minimum when the flue gas left the second combustion chamber.

## 4 Conclusions

The software Aspen Plus and Fluent were used to establish a mixed pyrolysis model and CFD model of the counter-flow rotary kiln incineration system, respectively. The effects of the operating temperature, hazardous waste calorific value, primary air velocity and primary air volume on the system operation effect were investigated. The main conclusions obtained are as follows.

- (1) As the operating temperature increased, the content of  $\text{SO}_x$  and  $\text{NO}_x$  gradually decreased, and the content of these two gas products tended to remain constant when the operating temperature of the counter-flow rotary kiln incineration system was greater than  $800\text{ }^\circ\text{C}$ . The result indicated that the incineration system should meet the condition of an operating temperature greater than  $800\text{ }^\circ\text{C}$ .
- (2) At an operating temperature of  $850\text{ }^\circ\text{C}$ , the incineration system was unable to meet its own heat balance through the combustion of hazardous waste when the calorific value of the hazardous waste was below  $1500\text{ kcal/kg}$ . Therefore, when using this incineration system for the incineration of hazardous waste materials, the hazardous waste should be simply screened according to the different calorific values.
- (3) The active air supply method helped to stabilize the operating conditions of the incineration system, but the primary air speed and the size of the primary air volume affected the actual operating effect of the incineration system. When the primary air volume and speed were too low, the mixed pyrolysis of the hazardous waste was not complete and the thermal reduction rate of the hazardous waste was not up to standard. When the primary air volume and velocity were too high, the temperature field in the kiln was not uniform and the temperature at the kiln head was too high. The simulation showed that the incineration system operated best at a wind speed of  $1.5\text{ m/s}$ , which corresponded to a primary air flow of  $5700\text{ Nm}^3/\text{s}$ .
- (4) The combustible gases generated in the rotary kiln were completely combusted in the secondary combustion chamber by means of  $\text{CH}_4$  make-up combustion. The temperature in the second combustion chamber could be made greater than  $1100\text{ }^\circ\text{C}$  by supplementary combustion, which met the industry requirements for controlling pollutant emissions.

**Acknowledgements** This work is supported by the National Key R&D Program of China (No. 2018YFC1902600).

**Funding** No funding to declare.

**Availability of data and materials** The data and materials are available.

## Declarations

**Competing interests** No competing interests to declare.

**Open Access** This article is licensed under a Creative Commons Attribution 4.0 International License, which permits use, sharing, adaptation, distribution and reproduction in any medium or format, as long as you give appropriate credit to the original author(s) and the source, provide a link to the Creative Commons licence, and indicate if changes were made. The images or other third party material in this article are included in the article's Creative Commons licence, unless indicated otherwise in a credit line to the material. If material is not included in the article's Creative Commons licence and your intended use is not permitted by statutory regulation or exceeds the permitted use, you will need to obtain permission directly from the copyright holder. To view a copy of this licence, visit <http://creativecommons.org/licenses/by/4.0/>.

## References

- Adrian VW, Cyrille V, Xavier C, Dominique G, Jacques P (2016) Extending refractory lifetime in rotary kilns for hazardous waste incineration. *Ceram Int* 42(15):17626–17634
- Adrian VW, Dominique G, Jacques P, Cyrille V, Xavier C (2021) Mullite–zirconia composite for the bonding phase of refractory bricks in hazardous waste incineration rotary kiln. *J Eur Ceram Soc* 41(1):995–1002
- Andréa PO, Itamar DS, Genésio J, Rogério JS (1998) Efficiency of destruction of waste used in the co-incineration in the rotary kilns. *Energy Convers Manage* 39(16–18):1899–1909
- Conner JR, Hoeffner SL (1998) The History of stabilization/solidification technology. *Crit Rev Environ Sci Technol* 28(4):325–396
- Hadas E, Mingelgrin U, Fine P (2021) Economic cost–benefit analysis for the agricultural use of sewage sludge treated with lime and fly ash. *Int J Coal Sci Technol* 8(5):1099–1107
- Huang CP, Dong C, Tang Z (1993) Advanced chemical oxidation: its present role and potential future in hazardous waste treatment. *Waste Manage* 13(5–7):361–377
- Ismail TM, Shi M, Xu J, Chen X, Wang F, El-Salam MA (2020) Assessment of coal gasification in a pressurized fixed bed gasifier using an ASPEN plus and Euler-Euler model. *Int J Coal Sci Technol* 7(3):516–535
- Lester TW, Cundy VA, Sterling AM, Montestruc AN, Jakway AL, Lu C, Leger CB, Pershing DW, Lighty JS (1991) Rotary kiln incineration: comparison and scaling of field-scale and pilot-scale contaminant evolution rates from sorbent beds. *Environ Sci Technol* 25(6):1142–1152
- Liu G, Chi Y, Jiang XG, Zhu J, Yan JH, Chen KF (2005) Mass transfer of simulative hazardous waste particles in rotary Kiln. *J Eng Thermophys* 02:343–346
- Makarichi L, Jutidamrongphan W, Techato K-A (2018) The evolution of waste-to-energy incineration: a review. *Renew Sustain Energy Rev* 91:812–821
- Malviya R, Chaudhary R (2006) Factors affecting hazardous waste solidification/stabilization: a review. *J Hazard Mater* 137(1):267–276
- Murphy AB, McAllister T (2001) Modeling of the physics and chemistry of thermal plasma waste destruction. *Phys Plasmas* 8(5):2565–2571

- Nanda S, Berruti F (2021) Municipal solid waste management and landfilling technologies: a review. *Environ Chem Lett* 19(2):1433–1456
- Paula O, De S, Josémenon JS (1998) Efficiency of destruction of waste used in the co-incineration in the rotary kilns. *Energy Convers Manage* 39(16–18):1899–1909
- Singhabhandhu A, Tezuka T (2010) The waste-to-energy framework for integrated multi-waste utilization: waste cooking oil, waste lubricating oil, and waste plastics. *Energy* 35(6):2544–2551
- Tekade RP (2021) The impact of hazardous waste and its impact on human health. *Int J Res Biosci Agric Technol*
- Visvanathan C (1996) Hazardous waste disposal. *Resour Conserv Recycl* 16(1–4):201–212
- Wajda A, Brociek R, Pleszczyński M (2022) Optimization of energy recovery from hazardous waste in a waste incineration plant with the use of an application. *Processes* 10(3):462
- Wang Z, Geng L (2015) Carbon emissions calculation from municipal solid waste and the influencing factors analysis in China. *J Clean Prod* 104:177–184
- Zhang S, Wang F (2022) Effect of interactions during co-combustion of organic hazardous wastes on thermal characteristics, kinetics, and pollutant emissions. *J Hazard Mater* 423:127209

**Publisher's Note** Springer Nature remains neutral with regard to jurisdictional claims in published maps and institutional affiliations.